Chapter 14

# Optimization and Improvement of Throwing Performance in Baseball Pitching Machine Using Finite Element Analysis

Shinobu Sakai and Hitoshi Nakayama

Additional information is available at the end of the chapter

http://dx.doi.org/10.5772/46159

## 1. Introduction

Pitching machines for baseball are widely used in venues ranging from professional baseball stadiums to amusement facilities (Adair, 1994). The most important purpose of the pitching machine is to reproduce the throws of an adversary pitcher, which will be useful for the improvement batting technique. The most common commercial pitching machines for baseball are the "arm" type and the "two-roller" type. Some pitching machines can pitch a high-speed ball (fastball) and a breaking ball, but these machines have certain limitations. In particular, it is very difficult to change ball speed and direction simultaneously (Mish et al., 2001). Therefore, the throwing performance of conventional pitching machines used for batting practice is not very high. Balls pitched to change in instant at various speeds and with different pitch types (ex. fastball, curveball, screwball and forkball) are easily achieved by a new pitching machine equipped with three rollers which has been developed by the authors. It is called a "three-roller" type pitching machine (Sakai et al., 2007). With the structure of three rollers, comes the production of a new pitching machine that can pitch balls repeatedly in the way the batter desires, controlling both ball speed and pitch type. However, as observed during our study, the seam of a baseball coming in contact with the rollers, the spin rate and projection angle of the ball delicately change. From the results, it became clear experimentally that from the throw accuracy deteriorates.

In this chapter, the throw simulation of the three roller-type pitching machine is analyzed using a commercial dynamic finite element analysis code (ANSYS/ LS-DYNA). The moving behavior (such as velocity and spin rate) and contact stress state of the ball pitched by the pitching machine are clearly observed. The effect of the throw accuracy by the seam posture of the ball in the machine is examined. In addition, the shapes and materials of the rollers do not

negatively affect the throw accuracy based on the seam posture examined. In other words, a robust roller (optimum roller) has been found. Furthermore, the optimum roller was produced on the specifications provided in the analytical results. Based upon throws from the machine using the rollers experimented on, the propriety of the analysis results is inspected.

## 2. Overview of commercial pitching machine

One important function of a pitching machine for baseball has traditionally been to throw a ball at a very high speed. The most common commercial pitching machines for baseball are the "arm" type and the "two-roller" type (Mish et al., 2001). The principal mechanism of the arm type machine is a spring and crank lever that imitates a human arm when pitching a ball (see Fig. 1(a)). The two-roller type is shown in Fig. 1(b). This machine uses two-roller to project a ball by taking advantage of the frictional force between the two rollers and the ball. Generally, the ball speed can be controlled with this type of machine, but direction changes are very difficult or impossible to achieve. With the two-roller machine type, the spin direction given to a ball is controllable only on the plane in which the roller is turning, because a ball flies only on that plane. This can change the spin rate and speed of the ball by changing the number of the ball's turns on its plane. However, the plane must be spun manually in order to produce arbitrary breaking balls. Additionally, the batter can be expected pitch type of a ball thrown by the two-roller type machine, because when a braking ball is pitched, the projection equipment (two rollers) in the machine must be slanted.

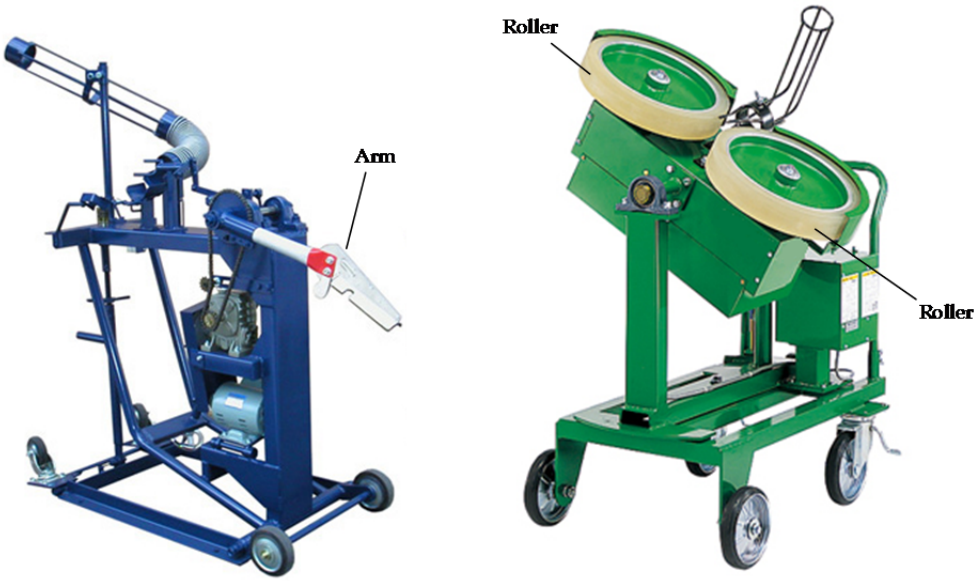


**Figure 1.** Commercial pitching machine. a) Arm type. b) Two-roller type.

Additionally, the throw performance of both types of pitching machine that have so far been developed for use during batting practice is not very high. The control precision of the latest commercial arm and two-roller types pitching machines is only 300 mm in height and 150 mm in width. One of the major reasons for this lack of precision is that baseball balls have a peculiar seam. Pitchers use this seam to throw various types of pitches, however this very seam also decreases the control precision of pitching machines (Mizota et al., 1995, Himeno et al., 1999, Sakai, et al., 2007).

If we wish to develop a high fidelity pitching machine for baseball capable of throwing a wide range of pitches with full freedom and control over both the speed and angular velocity of the ball, it is important that both of these quantities be independent of one another (Oda et al., 2003). Thus, the authors decided to develop a machine with the important functions (throwing freely and producing the breaking balls, speeds and direction a batter desires) that are currently missing from commercial pitching machines.

## 3. Overview of new type pitching machine

A new type of pitching consists of three rollers arranged around the circumference of a ball in its discharge position, and the rotary direction of the ball can be controlled over a full 360 degrees as the three rollers create three planes on a three-dimensional axis by variously changing the turn frequency of each roller. With this structure, various kinds of throws with variable pitch types and speeds, becomes possible. A schematic of the pitching machine that was developed by the authors is shown in Fig. 2(a), and a photograph of the machine is shown in Fig. 2(b).

This machine employs three rollers, which includes one more roller than the pitching machines typically found today. A ball for baseball is thrown with frictional force by the rubber tire, and this roller is installed around the circumference of a ball in its discharge position at 120° intervals. Three motors are installed, one in each respective roller, in which the number of revolutions can be adjusted from 0 to 3000 min-1, and these motors can be controlled independently. Additionally, this machine has a mechanism that can change the vertical angle $\Theta$ from -5° to 5° and the horizontal angle $\Phi$ from -6° to 6°, as shown in Fig. 2.

With the new type of pitching machine, which adopts these new mechanisms, a wide range of speeds (from 19.4 up to 44.4 m/s), pitch types (fastball, curveball or screwball) and variable directions, can be pitched as desired. Moreover, each motor is connected to a personal computer (PC) through a controller, and the number of revolutions of each of the motors can be controlled by the PC. In addition, this machine is equipped with various sensors that measure the number of revolutions $N_1$, $N_2$ and $N_3$ of three rollers, the vertical angle $\Theta$ the horizontal angle $\Phi$ and the initial velocity $V$ of the pitched ball. The pitching machine is capable of throwing a ball with higher accuracy (vertically 200mm and horizontally 100mm) in a wide area at a variety of speeds, employing different pitch types compared to current pitching machines.

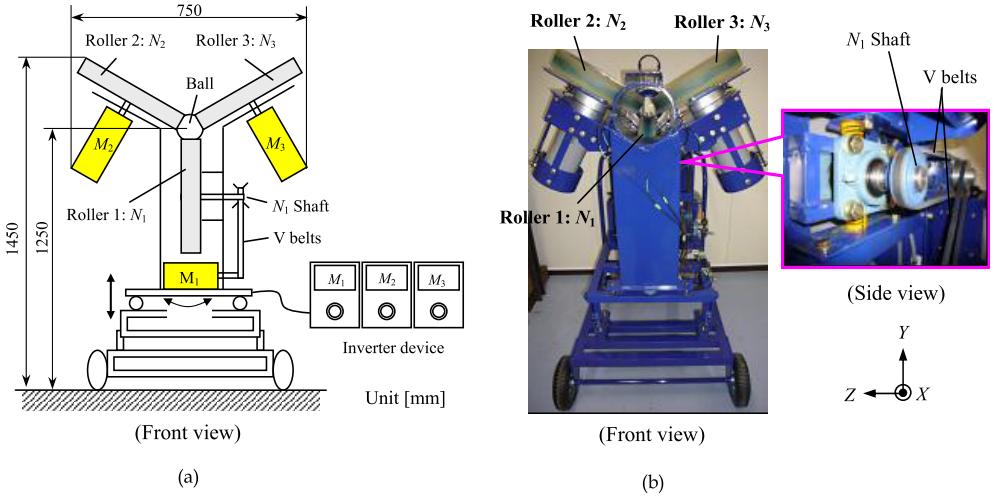


**Figure 2.** Three-roller type pitching machine. a) Schematic. b) Photograph.

## 4. Throw analysis of the three-roller type pitching machine

### 4.1. Finite element models and analysis conditions

In this study, the analysis models of only the roller parts and ball for baseball were made, because they were thought most important in the pitching machine for a thrown ball. Finite element models of a ball for traditional baseball and the roller part of the pitching machine with three rollers are shown in Fig. 3. Each of these measurements is shown in the figure. In this analysis, the aluminum alloy flange was very stiff compared to the ball and the rubber tire, and was treated as a rigid body. The ball was modeled with a viscoelastic agent in consideration of the dynamic characteristics of the ball. The characteristics of the ball were determined using a viscoelastic model of three elements, as shown in Fig. 4. This model shows the relationship between shear modulus $G(t)$ and time $t$, which are given in the following equation (Hendee et al. 1998, Nicholls et al., 2004, Sakai et al., 2008):

$$G(t) = G_\infty + (G_0 - G_\infty)e^{-\beta t} \tag{1}$$

where $G$ is the relaxed shear modulus, $G_0$ is the instantaneous modulus, and $\beta$ is the decay constant. Each material property in Eq. (1) was decided upon according to static and dynamic experiments and a finite element analysis (FEA) conducted on a ball. The material properties of these agents are shown in Table 1 (Nicholls et al., 2006). From the results of the analysis carried out beforehand, it was confirmed that the shape of the seam of the ball influences the throw more so than the materials of the ball. The seam of the ball has the same material properties as the ball's main body. The analysis for throwing the ball was calculated using dynamic finite element analysis code (ANSYS/ LS-DYNA, version 9.0, Theoretical Manual, 2002).

As a condition of the analysis, the initial velocity $V_0$=1.0 m/s and the initial angular velocity $\omega_0$ =28.56 rad/s of the ball are given for all cases. The termination time was set to 0.1s from the moment of impact of the rubber tire with the ball to the ball's ejection. These analysis conditions were calculated from the image with the pitching experiments filmed using a high-speed video camera. Here, the friction coefficient $\mu$ =0.5 was determined from the surfaces in contact with the ball and rubber tire. The value of $\mu$ will be described in the next section.

In general, there are two possible spin directions for each ball: two-seam (the seam appearing two times per ball rotation) and four-seam (the seam appearing four times). Additionally, a new model of a ball without a seam (a spherical ball) was created in order to examine the effect of the seam. In this analysis, there were three kinds of pitch type locations, which are simulated as shown in Table 2 (a no-spin ball, a fastball and a curveball). $N_1$, $N_2$ and $N_3$ were revolutions per minute for each roller, and the three roller numerical grand total was fixed at 4500 min-1. The analysis was intended to start from the time the ball was thrown to just after release. Also, the flight trajectory of the ball after release was not considered (Watts et al., 1975, Himeno, 2001, Mizota, 1995).

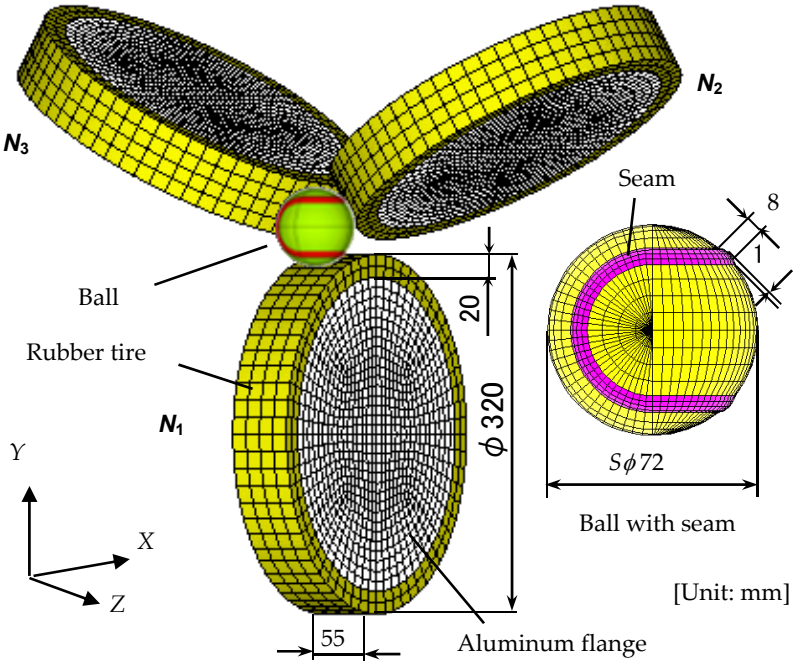


**Figure 3.** Finite element models of a ball with seams for baseball and three rubber rollers (15 104 elements).

In the analysis, a local coordinate axis was used as the starting point at the center position of a ball in release, as shown in Fig. 5. The projection vertical ($\theta$) and horizontal angles ($\phi$) were calculated by each ingredient of velocity $V$ ($V_x$, $V_y$, $V_z$) after the throwing of the ball.

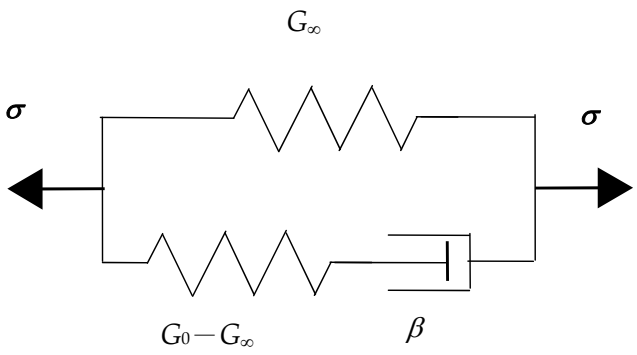


**Figure 4.** Viscoelastic model using three elements of the ball for baseball.

| Property | Rubber tire | Baseball |
|---|---|---|
| Density, $\rho$ (kg/m$^3$) | 1 000 | 835 |
| Young's modulus, $E$ (MPa) | 100 | — |
| Poisson's ratio, $\nu$ | 0.45 | — |
| Istantaneous modulus, $G_0$ (MPa) | — | 46.15 |
| Relaxed shear modulus, $G_\infty$ (MPa) | — | 8.85 |
| Bulk modulus, $K$ (MPa) | — | 100 |
| Decay constant, $\beta$ (s$^{-1}$) | — | 7 000 |

**Table 1.** Material properties of rubber tire and baseball (ball).

unit (min$^{-1}$)

| | $N_1$ | $N_2$ | $N_3$ | $N_1$+$N_2$+$N_3$ |
|---|---|---|---|---|
| Case 1 (No-spin ball) | 1 500 | 1 500 | 1 500 | 4 500 |
| Case 2 (Fast ball) | 1 700 | 1 400 | 1 400 | 4 500 |
| Case 3 (Curve ball) | 1 325 | 1 750 | 1 425 | 4 500 |

**Table 2.** Analytical conditions: three pitch types (no-spin ball, fastball and curveball).

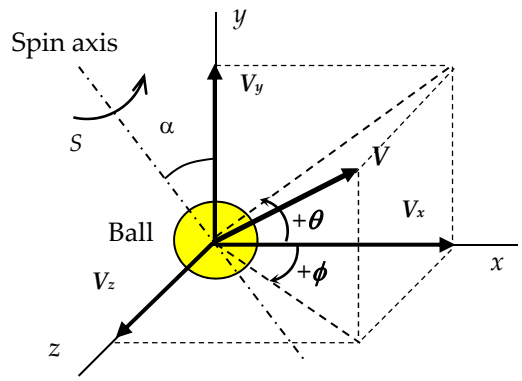


**Figure 5.** Coordinate system after pitching ball.

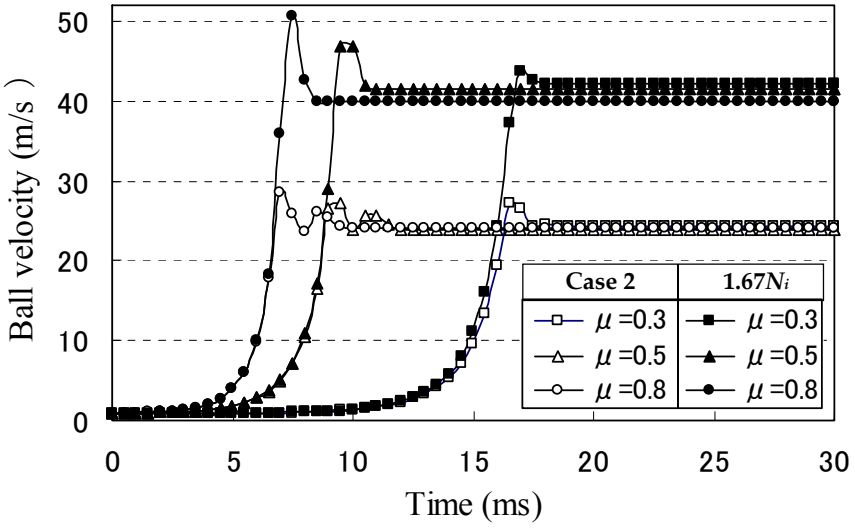


**Figure 6.** Time series of ball velocity $V_x$ for four-seam fastball (case 2) after pitching.

## 4.2. Coefficient of friction μ between ball and three rollers

The value of the coefficient of friction $\mu$ range of 0.3-0.8 was analyzed. The results from letting $\mu$ for the three-roller type pitching machine vary between 0.3, 0.5 and 0.8 are shown in Fig. 6. This figure shows a time series for the $x$-direction velocity of a ball ($V_x$) in case 2 (four-seam fastball), and three rollers exhibited 1.67 revolutions. As a result, when the ball came into contact with the rollers, the velocity of the ball suddenly increased.

Conversely, it is understood that a pitched ball maintains a contact speed after its release without regard for value of $\mu$. For this reason, the ball is in a slippery state during the early stages of its contact with the rollers, and contact time changes with changes in the value of $\mu$.

In the moment that the rollers pitches to hold the ball, the contact state of the ball and rollers almost becomes an adherence state in the whole area. Therefore, the ball's course does not vary with the value of $\mu$. From the results, the coefficient of friction $\mu$ was determined to be 0.5 (Sakai et al., 2007, Nicholls et al.,2004).

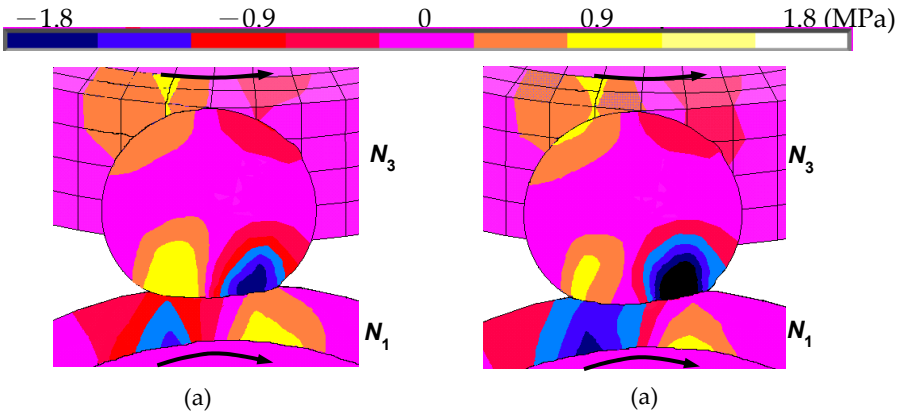


**Figure 7.** Shear stress distribution in $x$-$y$ section of a pitched ball. a) No-spin ball. b) Fastball.

### 4.3. Analysis results and discussion

One example of the analysis results, the shear stress distribution in an $x$-$y$ section of a pitched two-seam ball is shown in Fig. 7. In the figure, (a) and (b) show the pitch of a no-spin ball and fastball, respectively. It is understood that the absolute value for the fastball is more than the no-spin ball. For this reason, the number of turns of the $N_1$ roller is faster than other rollers in order to add back spin to a ball for the fastball. The shear stress values in the occurred contact surface neighborhood with the ball and the $N_1$ roller therefore becomes high.

A time series of the ball's $x$ direction velocity $V_x$, when the two-seam ball was thrown by the three pitch types (no-spin ball, fastball and curveball) is shown in Fig. 8. The velocity-time curve was almost the same for all the pitch types. The ball's velocity suddenly rises when the ball begins to come into contact with the roller, and is pitched at an almost constant speed after release. However, while not shown here, this is almost the same as the other pitch types and different seam postures. The speed of a pitched ball was understood not to be influenced by the pitch type. Additionally, when the number of a roller is $n$, the outside radius of a roller is $R$ (m), the relationship between the number of revolutions of each roller $N_i$ (min-1) and the ball's speed $V$ (m/s) can be given by the following equation:

$$V = \frac{\sum_{i=1}^{n} VR_i}{n} = \frac{2\pi R}{60n} \sum_{i=1}^{n} N_i \tag{2}$$

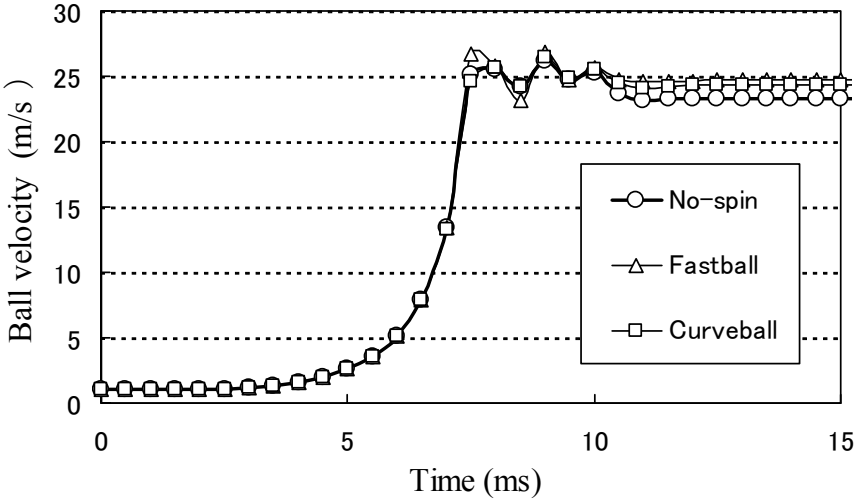


**Figure 8.** Time series of ball velocity $V_x$ in two-seam ball during release

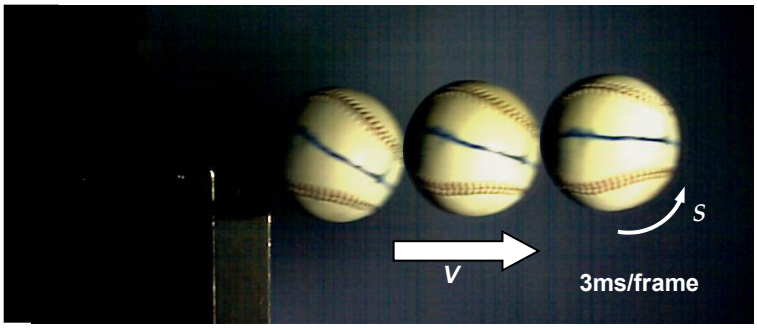


**Figure 9.** Flight behavior of ball after release using high-speed video camera in Case 2 (Fastball, $V$ = 25.1 m/s.

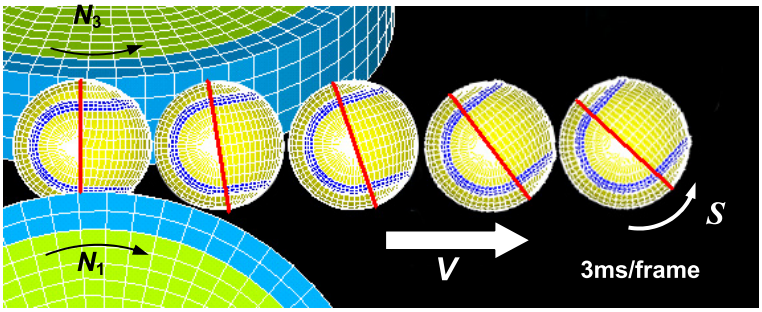


**Figure 10.** Flight behavior of ball after release by FEA result in Case 2 (Fastball, $V$=24.7 m/s).

### 4.4. Comparison of results of throw experiment and analysis

The three-roller type pitching machine shown in Fig. 2 was used, and it was tested to throw a ball in the throw condition shown in Table 2. The state of the throw experiment filmed the behavior of the ball just after release at intervals of 2000 fps (frames per second) using a high-speed video camera (MEMRECAM fx-K3, made by nak Image Tech. Inc.). One example of the throw experiment results, a flight image of the pitch of a four-seam fastball, is shown in Fig. 9 (Nicholls et al., 2003, Chu et al., 2006, Sakai et al., 2007, Takahashi et al., 2008). As well, a state of the flight of the FEA that pitches the ball in the same condition in Fig. 10 is shown.

From both figures, the spin axis of the ball is the axis which is inclined to wards the *Z*-axis (side of a paper plane) from the vertical direction. It is understood that the ball is pitched spinning around its axis. The speed of the pitched ball *V* and spin rate *S* were calculated from both images. The experimental and analytical values were almost the same. Additionally, similar results were acquired in the experiments and the simulation (FEA) of other pitch types and seam postures. These results showed good agreement between the experiments and the FEA.

Figure 11 shows the comparison of the spin rate *S* of each pitch type when we threw a ball with two- or four-seams in the experiments, as well as the analysis results. The spin rates of the experiment and analysis values are understood to be almost the same in both pitch types. Additionally, a pitch type is decided by the number of turns of the three rollers. It is understood that there are few differences associated with seam posture (Jinji, 2006).

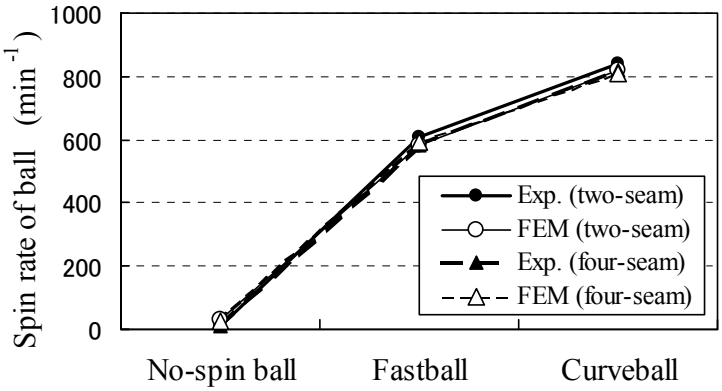


**Figure 11.** Spin rate of ball after throw for three pitch types.

Figure 12 shows the comparison projection horizontal angle $\phi$ after a throw of each pitch type. From the results, it is understood that the experiment and analysis values are different by pitch type and seam posture. In this case, the analysis and the experiment values were each compared with each seam posture (two- and four-seam), and the absolute experimental value was slightly greater than the analysis one within the three pitch types. Also, it is understood that both values become almost equal with minor differences.

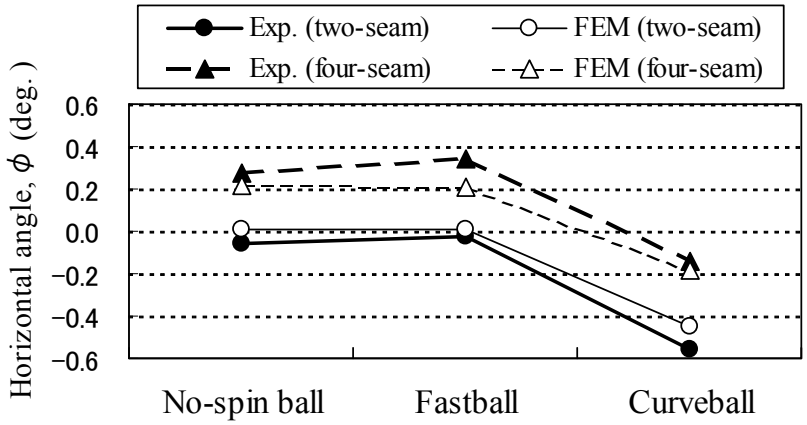


**Figure 12.** Horizontal angle $\phi$ of ball after throw for three pitch types.

Conversely, the difference in value between the two- and four-seam balls in the experiment was from 0.3 to 0.4 degrees for each pitch type. Here, in this throw condition (the initial ball-velocity 25m/s), when a difference of $\phi$ was 0.2 degrees, the trajectory of the pitched ball to a home plate is about 70mm (the size of one ball) slip off in the side direction in theory. This difference is thought is a significant factor contributing to the fall in throw accuracy by the seam of a ball for baseball (Frohlich, 1984, Mehta, 1985, Watts et al., 1975, Mizota et al., 1995, Alaways et al., 2001).

From the results of the throw experiments and simulations, the value of the speed, spin rate and projection angle in the pitched ball are almost the same. It is thought that the analysis model and its results are proper.

## 5. Analysis of models that changed roller outer diameter, *D*

### 5.1. Analysis models and conditions

The roller outer diameter $\phi$ 320mm (standard model; D320) for the present experiment was changed, the analysis models of $\phi$ 220mm (D220) and $\phi$ 420mm (D420) were made the roller of the small and large diameter. Both the analysis models are shown in Figs. 13 and 14, respectively. Here, the roller materials and roller distance are the same as the analysis model in the previous section.

In the analysis conditions, the speeds and pitch types of the pitched balls are the same as in the standard model D320. The circumference velocity $VR_i$ of each roller was calculated from the number of each roller turns as shown in Table 2.

Next, the number of each roller turn $N_i$ (min-1) was calculated so that $VR_i$ in the case of D220 and D420 became equal. Both the models were set to the number of those turns. Additionally, the initial velocity of the ball was the same as stated in the previous section, and the throw analysis was then carried out.

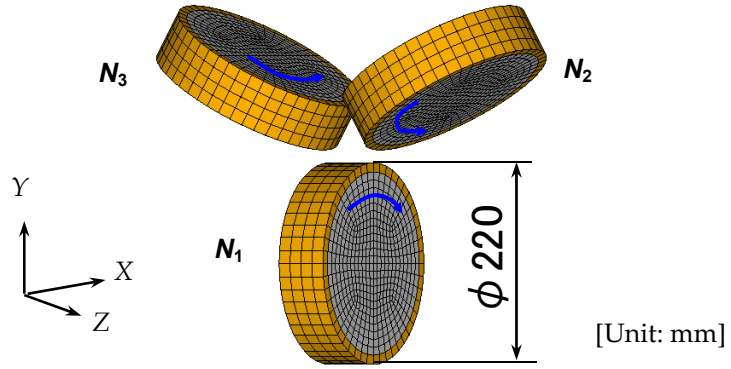


**Figure 13.** Finite element models of small rollers (D220).

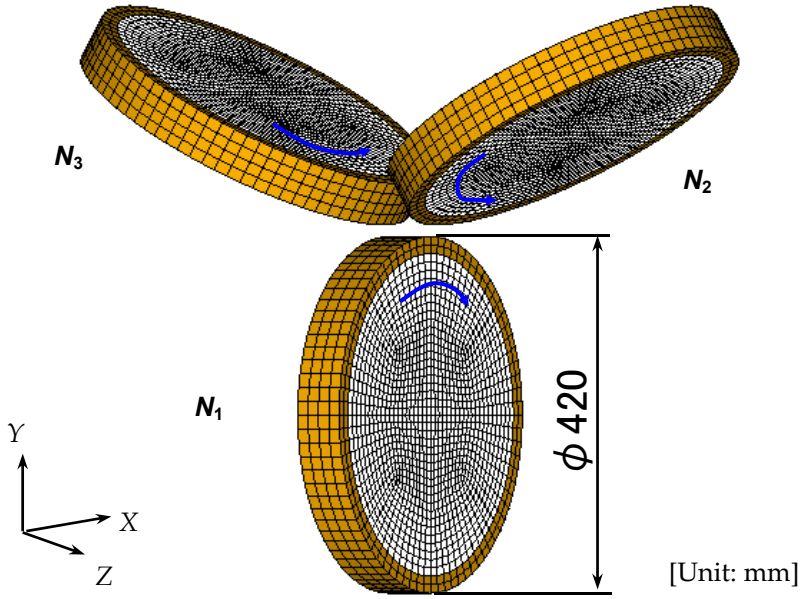


**Figure 14.** Finite element models of large rollers (D420).

## 5.2. Results and discussion

One example of the analysis results, the time-history of a two-seam fastball's velocity for each model, is shown in Fig. 15. The number of three rollers turn of each model increased to 1.67 times (ex. D220H), is shown in the same figure. As shown in the figure, there is a small difference in the time at which the ball comes into contact because each roller's the diameter was different. A similar velocity-time curve is drawn for all the models.

Otherwise, the speed of a pitched ball after the throw was almost constant in all models. This is not shown here. This result was identical to when a four-seam ball was thrown. The ball speed was decided almost entirely by the circumference velocity of the roller, and clearly does not depend on the roller's outer diameter.

Figure 16 shows the comparison of several rollers on the spin rate in two-seam balls. The spin rate of the pitched curveball in D220 is compared with other models that are slightly lower. It is understood that the spin rate in D320 and D420 is almost equal for all pitch types. The spin rate is an important factor in deciding a pitch types (breaking balls), because the throw performance of the D220 is lower in comparison with other rollers.

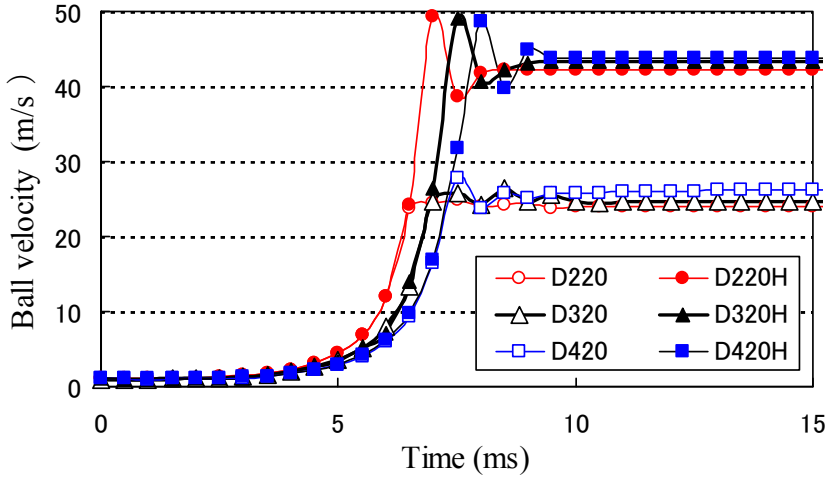


**Figure 15.** Time series of ball velocity for two-seam fastball during release on several rollers *D*.

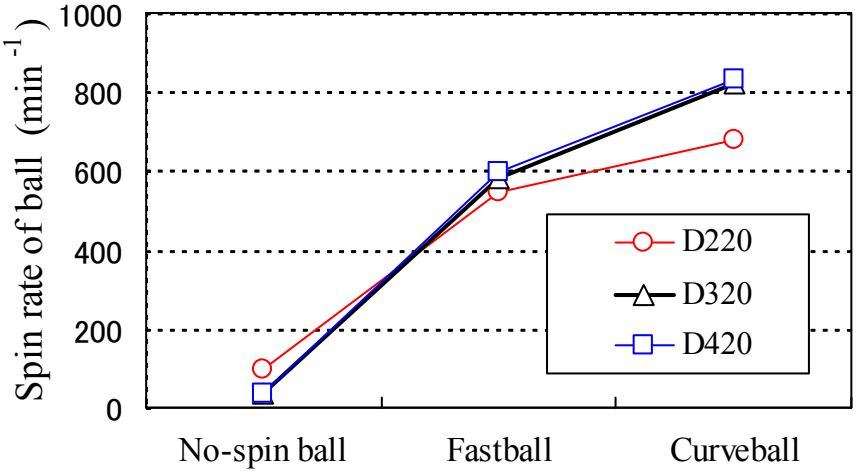


**Figure 16.** Comparison of several rollers on spin rate of two-seam ball.

Next, throw accuracy by seam posture was evaluated quantitatively. A difference of a vertical and horizontal projection angles $\theta$ and $\phi$ after a ball is thrown is defined as $\Delta\theta$ and $\Delta\phi$ in the next two equations, respectively:

$$\Delta\theta = \left| \theta_2 - \theta_4 \right| \tag{3}$$

$$\Delta\phi = \left| \phi_2 - \phi_4 \right| \tag{4}$$

where the suffix 2 or 4 expresses two- or four-seam balls, respectively. If the values of $\Delta\theta$ and $\Delta\phi$ are small, the throw accuracy of the pitching machine is higher with respect to the seam position and posture.

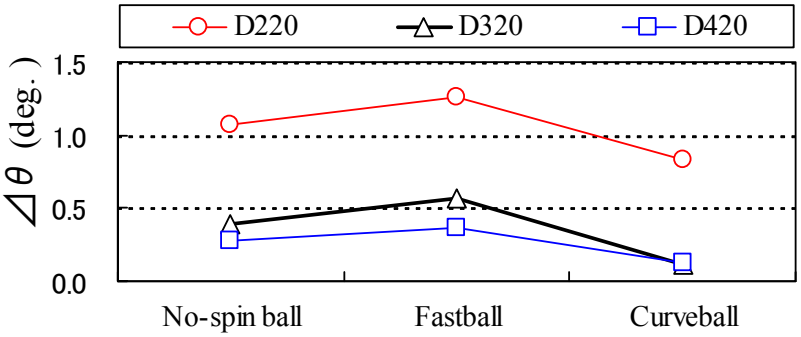


**Figure 17.** Comparison of several rollers on $\Delta\theta$.

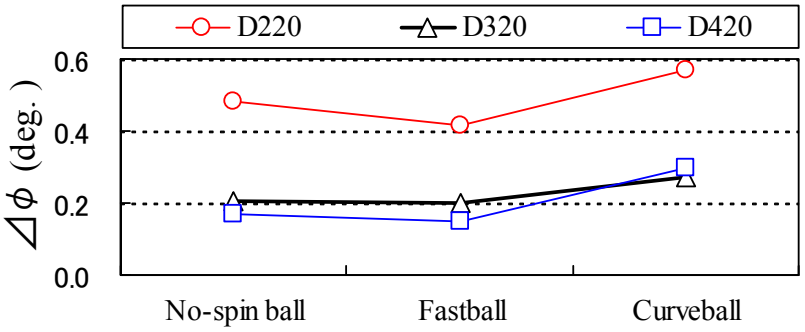


**Figure 18.** Comparison of several rollers on $\Delta\phi$.

Figures 17 and 18 compare $\Delta\theta$ and $\Delta\phi$ for each model when pitched respectively for each pitch type. In the case of the fastball pitch, in comparison with other pitch types, it is understood that its value in all models is the largest. In the case of the compared models, the value of $\Delta\theta$ in D220 is bigger for all pitch types, and it is understood that D320 and D420 are smaller. Conversely, the value of $\Delta\phi$ in the curveball tends to become slightly larger than other pitch types without relation to the model. $\Delta\phi$ is smaller, so the roller diameter becomes bigger. Additionally, it is understood that there is not any difference in D320 and D420.

From the results of the throw analysis where the roller diameter *D* was changed, the spin performance and the throw accuracy are poor in D220 and the outer diameter is small. It is understood that the performance of D420, with the largest outer diameter, was the best.

In general, a roller with a big diameter is used, a motor capable of producing a large output becomes necessary. In this case, the pitching machine in itself becomes large-scale, and its gross weight increases. However, if such problems can be solved, in terms of throw accuracy, it is advantageous to make the diameter of the roller larger.

When these things are considered generally, there are a few differences regarding the throw performance of the D420 and D320. The roller diameter of the three-roller type pitching machine is regarded as the measurement that used $\phi$320mm present are practical.

## 6. Analysis of models that changed radius of roller distance, *r*

### 6.1. Analysis models and conditions

A roller-type pitching machine is a machine in which a ball is picked up by the roller, and is thrown. The performance of roller-type pitching machines changes based on the radius *r* of each roller. Thus, the roller distance of the present machine (D320, radius *r* =25.1 mm) was as shown in Fig. 19. The roller distance of the models was analyzed which may have been narrow or broad. Also, the throw analysis was the same as in the previous section.

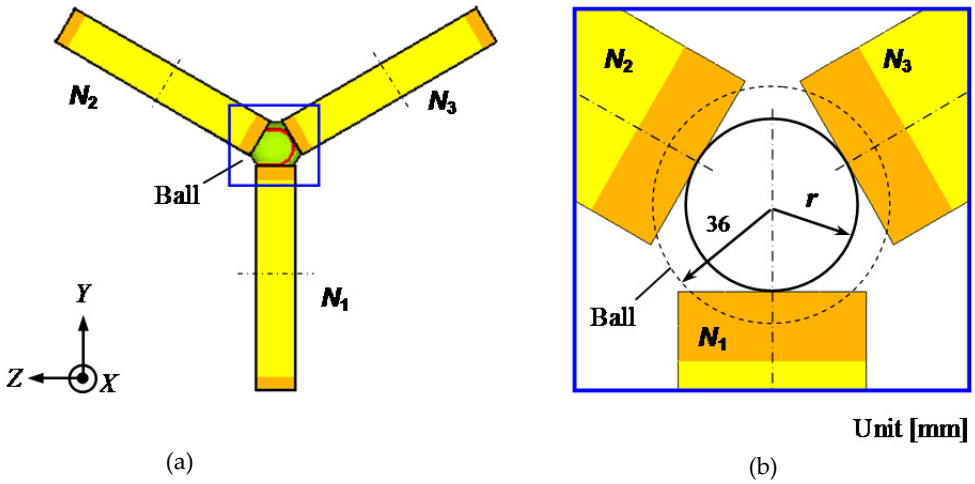


**Figure 19.** Radius of each roller distance, *r* a) Ball and three rollers. b) Close-up view.

### 6.2. Results and discussion

One example of the analysis results, the velocity of two- and four-seam fastballs of each model, is shown in Fig. 20. In this figure, the ball speed is understood to not be influenced

by the seam posture in any of the cases. Additionally, the speed of the pitched ball is fixed at about 25m/s within the range of 23.1mm < $r$ < 27.1mm. The speed rises with increases in $r$, and the greatest speed was approximately $r$ = 31.1mm. The ball speed suddenly decreases when $r$ > 31.1mm. It is thought that the ball is not held strongly enough between the rollers when $r$ > 31.1mm. Figure 21 shows the relationship between $\Delta\theta$, $\Delta\phi$ and $r$ from the analysis results. It is understood that $\Delta\theta$ is at its minimum value at 0.19 degrees when $r$ =33.1mm, and $\Delta\phi$ is moves towards its minimum value at 0.10 degrees when $r$ = 27.1mm.

From these results, when the speed of a pitched ball thrown from a three-roller type machine is considered, it is thought that the radius of a roller distance $r$ in the range of 23.1mm < $r$ < 33.1mm is practical. If $r$ is limited to this range, the throw accuracy becomes highest at approximately $r$ = 27.1mm when $\Delta\theta$ and $\Delta\phi$ are both at their minimum values.

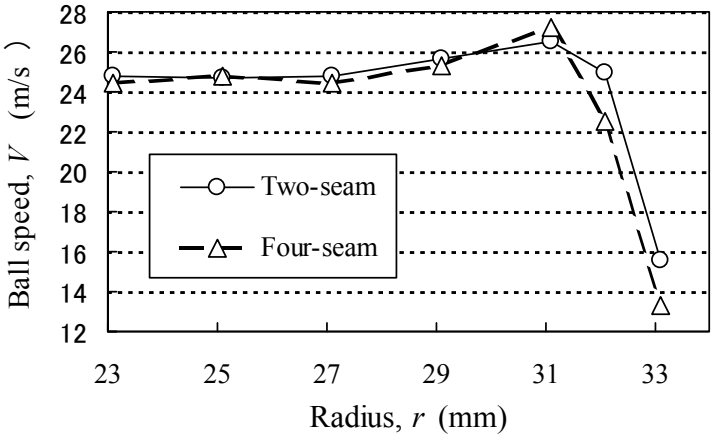


**Figure 20.** Relationship between ball speed and of each roller distance, $r$.

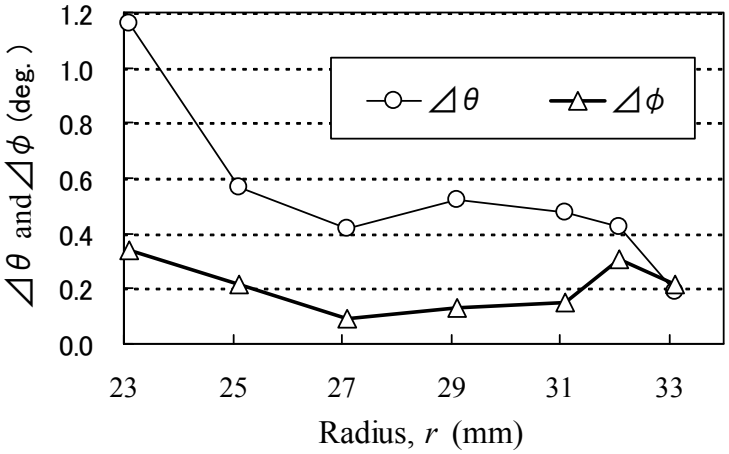


**Figure 21.** Relationship between $\Delta\theta$, $\Delta\phi$ and of each roller distance, $r$.

In theory, the control accuracy of the pitched ball by a pitching machine in this case is entered in the vertical and horizontal errors at 140mm and 50mm, respectively. Therefore, the measurements needed to create a new type of pitching machine have been achieved. (Mizota et al., 1995, Himeno, et al., 1999, Nathan, 2008).

## 7. Throw analysis changed roller shape

### 7.1. Analysis models and conditions

In order to throw a two- or four-seam ball, it is necessary to prepare the posture of the ball artificially. Thus, the roller developed by us shows that the throw accuracy is not affected by a seam and its posture (the robustness roller). We let the shape change in the roller section. Above, the roller section used was a flat type roller (flat roller) of a rectangle. For the concave type roller the central part of which where the ball touched became hollow (see Fig. 22), while the convex type roller which swelled (see Fig. 23) were devised. The radius of curvature $R$=100mm, and the distance from the center to the outside surface of the roller (the radius of each roller distance) was $r$=25.1mm in both models.

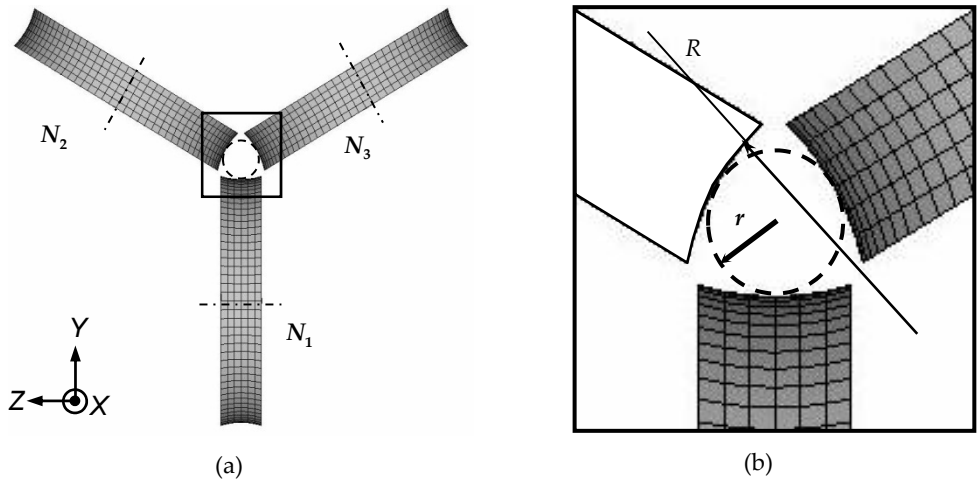


**Figure 22.** Concave type roller. a) roller shape. b) Close-up view.

### 7.2. Analytical results and discussion

The analytical results of a pitched fastball are shown in Figs. 24, 25 and 26. Figure 24 shows a time series of the two-seam ball's velocity. The velocity-time curve was almost the same for all roller types. The ball's velocity suddenly rises when the ball begins to come in contact with the roller, and is pitched at an almost constant speed after release. However, while not shown here, this is almost the same as other pitch types and different seam postures. The speed of a pitched ball was understood not to be influenced by the roller shape.

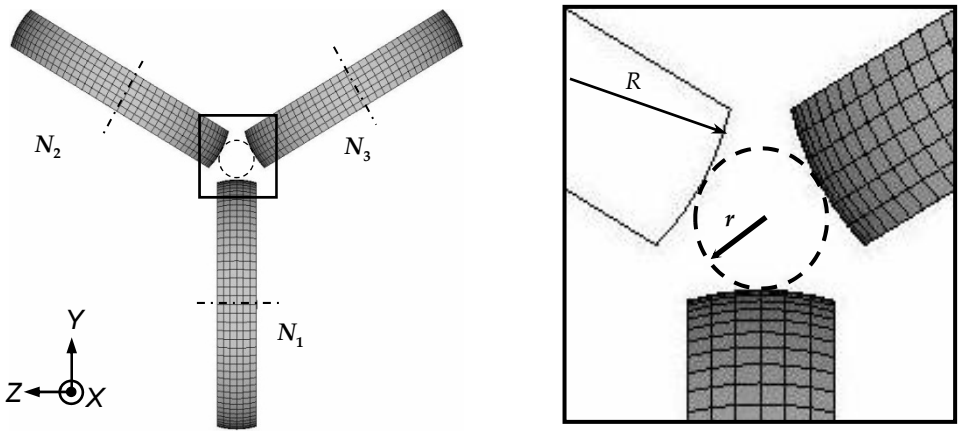


**Figure 23.** Convex type roller. a) roller shape. b) Close-up view.

On the other hand, the difference of the vertical angle $\Delta\theta$ (see Fig. 25) and horizontal angle $\Delta\phi$ (see Fig. 26) with several rollers in the fastball pitch changed based on seam posture and roller shape dramatically. In both figures, it is understood that the variation in the range of the convex type roller by seam posture was smaller than the other roller types. Here, the value of difference of both seams (two- and four-seam) was small, meaning that the throw accuracy is higher.

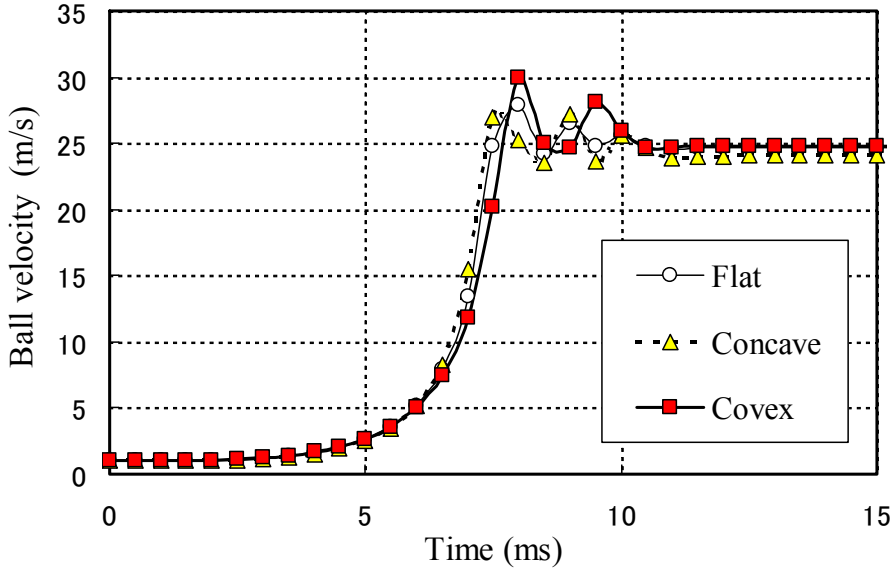


**Figure 24.** Time series of the ball velocity with several rollers for two-seam fastball.

In particular, the value of difference of horizontal angle $\Delta\phi$ becomes a factor of a pitch which hits the batter in an actual baseball game. Therefore, the value of $\Delta\phi$ of a commercial pitching machine is an important factor in the throw accuracy. The throw accuracy of the convex type roller is higher than the flat and concave type rollers.

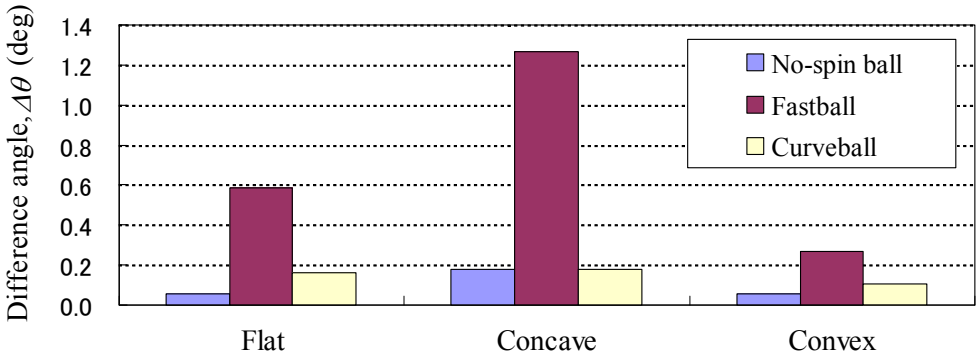


**Figure 25.** Difference of vertical angle $\Delta\theta$ with several rollers for three pitch types.

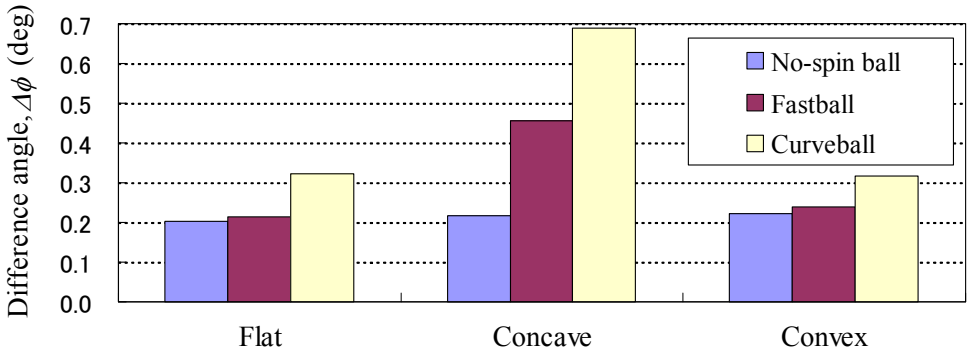


**Figure 26.** Difference of horizontal angle $\Delta\phi$ with several rollers for three pitch types.

## 8. Optimum design of roller

### 8.1. Optimization problems of roller

From the results in the previous section, when the roller shape is changed into convex from a flat design, the throw accuracy may become higher than the existing the flat type roller. In this section, the dynamic finite element analysis (FEA) is used, and the optimum design of the roller improving the throw accuracy is tried. Young's modulus $E$ of the roller, the radius of curvature $R$ and the radius of each roller distance $r$ are the three design variables in Fig. 23. There is the optimization problems in designing rollers that have a different projection angle formed by differences in the seam posture becoming the smallest.

## 8.2. Response surface method and optimization

In order to obtain the optimum design, as evaluation of the roller optimization corresponding to the design variables, a difference of the projection horizontal angle ($\Delta\phi$) according to the two- and four-seam postures was decided upon. Objective function $f_\phi$ uses a difference of an argument regarded as most important to the throw accuracy. $f_\phi$ is minimized so that the effect of the seam becomes small, as in the equation given below:

$$Minimize \quad f_\phi = \Delta\phi + \eta \tag{5}$$

where $\eta$ is a penalty coefficient. In the case of minimal spin rate $S$ (min-1), not all pitch types are thrown. Thus, this consideration was removed from the optimum solution. It is prescribed in the next condition:

$$\left.\begin{array}{ll} S_2 \geq 400 \; and \; S_4 \geq 400 & \rightarrow \; \eta = 0 \\ S_2 < 400 \; or \; S_4 < 400 & \rightarrow \; \eta = 1 \end{array}\right\} \tag{6}$$

where 2 and 4 indicate the two-seam and four-seam, respectively. Eq. (5) is derived by using Response Surface Methodology (Myers et al., 1995, Khuri et al., 1996). The response surface is built by using a response surface tool: RSMaker for Excel (Todoroki, 2010). The response surface dispersion is shown in the standard three design variables ($R$, $r$, $E$) in Table 3. All analyses for 3×3×5 (45 ways) in Table 3 were executed. Additionally, the pitch type decided on was the curveball, because the change of the projection horizontal angle $\phi$ is the biggest over the other pitch types from the analytical results in the previous section.

| Radius of curvature $R$ [mm] | Center distance $r$ [mm] | Young's modulus $E$ [MPa] |
|---|---|---|
| 36 | 22.1 | 10 |
| | | 20 |
| 72 | 25.1 | 50 |
| | | 100 |
| 100 | 30.1 | 500 |

**Table 3.** Design variables (1st analysis).

| Radius of curvature $R$ [mm] | Center distance $r$ [mm] | Young's modulus $E$ [MPa] |
|---|---|---|
| 100 | 24.1 | 30 |
| | 24.6 | 40 |
| | 25.1 | 50 |
| | 25.6 | 60 |
| | 26.1 | 70 |
| | | 80 |

**Table 4.** Design variables (re-analysis).

From the results, many peaks are recognized by the provided response values, and it was difficult to provide similar accuracy in all design domains. Thus, the response surface by the interpolation calculation was made, and the optimum point candidate was predicted. One example of the response surface made in interpolation calculation using the graph software ORIGIN is shown in Fig. 27 ($E$=50MPa). It is predicted that the optimum point for $r$=25mm and $R$=100mm. It is observed once again in the surrounding region that the zoomed response surface is made, and the optimum point is found in the small region. In the re-analysis, $R$ was fixed at 100mm, the design variables were the two $r$ and $E$ (cf. Table 4). The reason for this is because sensitivity for the objective function was sensitive both to $r$ and $E$ in the range of $R$>72mm.

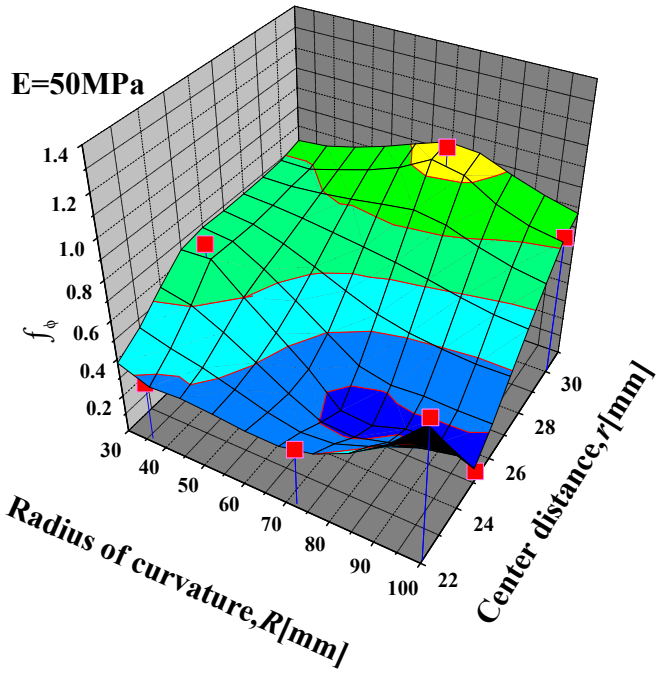


**Figure 27.** Response surface of interpolation calculation for curveball ($E$ =50MPa).

The enlarged response surface demanded by the third multinomial expression approximation and the optimum point (seal ○) are shown in Fig. 28. In this way, the optimum condition of the convexity roller ($r$ =25.4mm, $E$ =52.4MPa) was pursued. Additionally, the re-analysis was executed in these conditions once again, and it was confirmed that these values are the optimum values. From Fig. 28, it is understood that the optimum point neighborhood is a gentle curved surface and range.

Next, when the pitch type was changed mid-pitch from a fastball to a curveball, roller geometry was optimized such as for the curveball. The zoomed response surface for the fastball is shown in Fig. 29 (seal ○ is the optimum point in the curveball). The changed

values of both design variables are small in comparison with the curveball. Also, the optimum point was almost the same as the value pursued in the curveball.

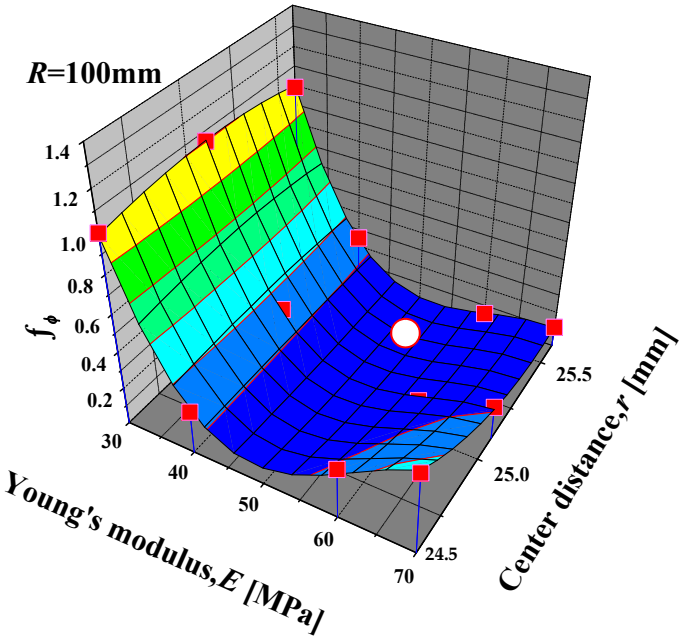


**Figure 28.** Zoomed response surface and optimum solution for curveball ($R$ =100mm)

We think that the optimum value provided by the curveball is close to the optimum value of other pitch types.

### 8.3. Throw experiment using optimized convex type roller and throw accuracy evaluation

In the previous section, the optimum condition of the convex type roller was decided. The proprieties of these analysis results are examined. The convex type roller pursuing the optimum condition has been produced, and the pitching machine using its rollers was tested to throw the ball. The convex type roller produced the shape geometry that is the radius of curvature $R$=100mm and rubber as a soft material (Young's modulus, $E$ =52MPa). This is called the soft convex type roller. In Fig. 23, it was a set of three of these rollers, and it was adjusted to become the center distance $r$=25.4mm.

The state of the throw experiment filmed the behavior of the ball just after release at intervals of 2000 fps using the high-speed video camera. For comparison of the roller shape, the produced soft convex type roller was filmed. The throw condition was experimented on in the same way as the analysis shown in Table 2, in order to compare it with the FEA.

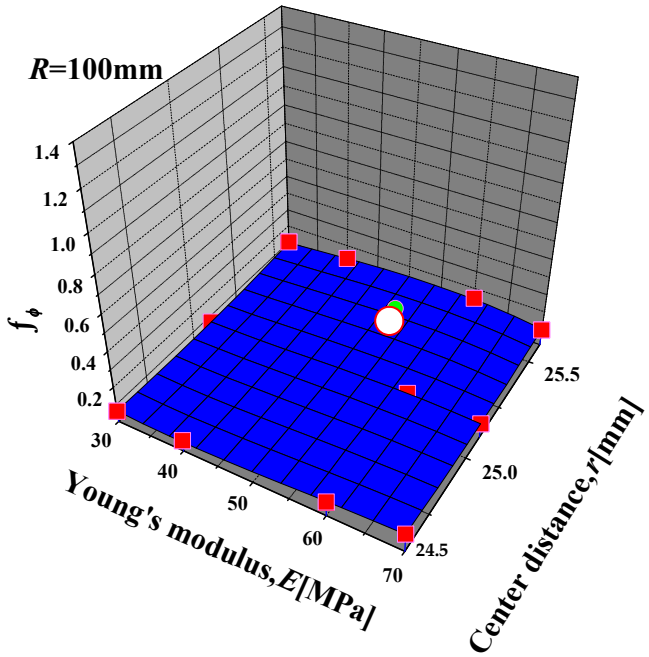


**Figure 29.** Zoomed response surface and optimum solution for fastball ($R$ =100mm)

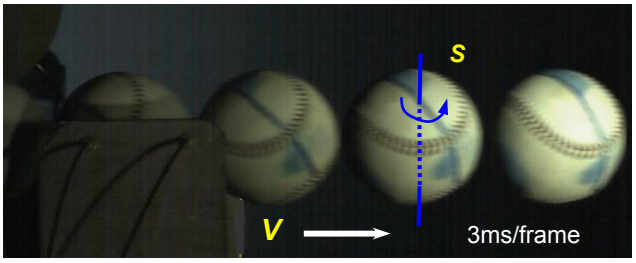


**Figure 30.** Flight behavior of ball after release using high-speed video camera for four-seam curveball by convex roller ($V$=25.3 m/s, $S$=820min-1).

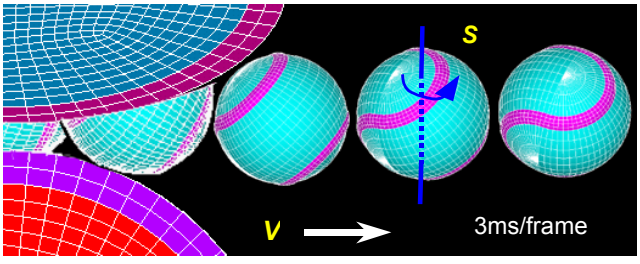


**Figure 31.** Flight behavior of ball after release by FEA results for four-seam curveball by convex roller ($V$=24.9 m/s, $S$=810min-1).

One example of the throw experiment results with the soft convex type roller, a flight image of the pitch of a four-seam curveball, is shown in Fig. 30. Otherwise, a state of the flight of the FEA that pitches a ball in the same condition in Fig. 31 is shown. From both figures, the spin axis of the ball is the axis which is inclined to the *Z*-axis (side of a paper plane) from the vertical direction. It is understood that the ball is pitched spinning around its axis. The speed of a pitched ball *V* and number of spins *S* were calculated from both images. The experimental and analytical values were almost the same. Additionally, similar results were acquired in the experiments and the simulation (FEA) of other pitch types and seam postures. These results show good agreement between the experiments and the FEA.

Figure 32 compares the roller geometry of the experiment and analytical values of the balls' speed *V* for the two pitch types (fastball and curveball) using the four-seam ball. It is understood that the balls' speed in the convex type roller increases a little more than in the flat type roller without a relation to pitch types. Its velocity increases by about 3%. These results are the same as the former FEA results (cf. Fig. 24).

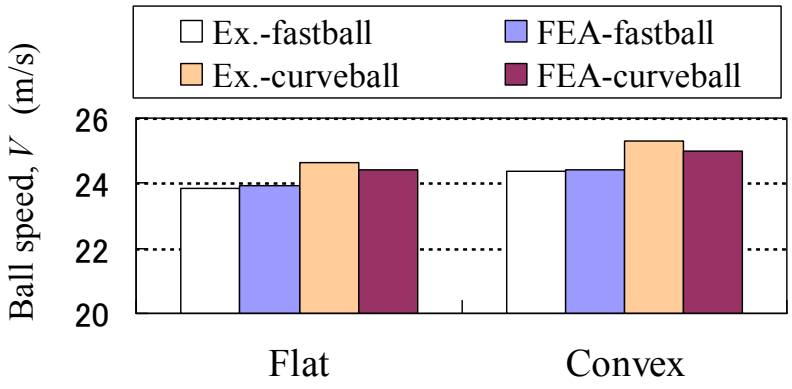


**Figure 32.** Comparison of roller geometry on ball speed *V* for four-seam ball after pitching.

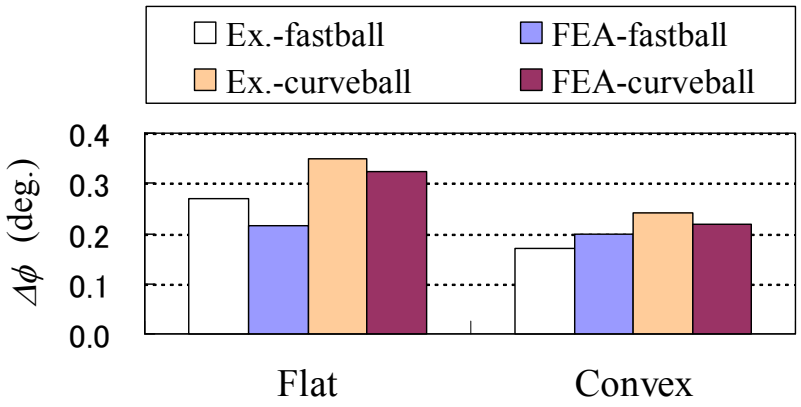


**Figure 33.** Comparison of roller geometry on the difference of horizontal angle $\Delta\phi$

Additionally, the experiment and analytical values were compared for roller geometry. The experimental and analytical values were almost the same. It was identified that the reproduction of the throw of the ball was experimented on several times.

On the other hand, the difference of the projection horizontal angle ($\Delta\phi$), which is one of the important performance considerations of a pitching machine, was considered in order to evaluate the throw accuracy of the machine by the seam posture quantitatively. If the value of $\Delta\phi$ is small, the throw accuracy of the pitching machine is higher with respect to the seam position and posture. The fastball and curveball were thrown using the two- and four-seam balls, respectively, and the projection horizontal angle $\phi$ was measured for each pitch type. The throw experiments were tested with two kinds of rollers of the flat and soft convex types.

Figure 33 shows the difference of $\Delta\phi$ values which were calculated in Eq. (4) from the values measured in these experiments. The values of the FEA in the throw condition are the same as the experiment shown in the figure. The values of the experiments were compared with the roller shape. The convex type roller showed smaller values than the flat type regardless of pitch type. The convex type roller was affected by the improvement in throw accuracy.

Finally, the analysis accuracy was described. In Fig. 33, each ball type is shown, and the $\Delta\phi$ of the analysis and experiment are compared, respectively. This included some errors which the experiment values (less than 0.07 degrees) considered. It is thought that the analysis accuracy is high enough. From these results, the validity of the computational model and its results in this study were confirmed.

## 9. Conclusion

In this chapter, the throw simulation using the finite element analysis (FEA) and experiments analyzed the improvement in the throw accuracy of three-roller type pitching machines for the purpose of studying the effect of the seam on the behavior and throw accuracy of the ball. The analytical models of the changes in the outer diameter, the distances and the form of the roller were made. The roller based on the convex shape was suggested, and the materials and the shapes of its roller were optimized. Additionally, throwing the ball using its optimized roller was experimented on, and the propriety of the analysis results was inspected. The conclusions provided are as follows:

1. In the roller type baseball pitching machine, the seam of a ball does not influence the ball's speed or spin rate after release, while the effects of the seam on the projection angles $\theta$and $\phi$ vary.
2. The throw accuracy of the three-roller type pitching machines was improved through the utilization of a larger roller diameter.
3. In the case of the flat roller, the radius of the three-roller distance is 27.1mm, the seam of a ball increase, and the throw accuracy of the pitching machine is improved.
4. The soft convex type roller ($R$=100mm and $E$=52.4MPa), which is the optimized roller, does not have an affect on the seam of a ball, and the throw accuracy and robust are high.

## Author details

Shinobu Sakai*
*School of Mechanical Engineering, Kanazawa University, Japan*

Hitoshi Nakayama
*Development Division, Sunaga Kaihatsu Co., Ltd., Japan*

## Acknowledgement

Great assistance was given to this study by Mr. Yuichiro KITAGAWA and Hirotoshi KAKUDA, who were seniors at this university while it was being conducted. For their help in making the finite element models and test of the machine, the authors wish to express great thanks. Additionally, concerning the three-roller type pitching machine described. Here, including the structure and control method, Japanese patent applications (No. 2001-45941 and No. 2007-301892) have already been filed at the Japan Patent Office.

This work was supported by Grants-in-Aid for Scientific Research (Grant No. 24560255) from the Ministry of Education, Culture, Sports, Science & Technology (MEXT) in Japan. The authors would like to thank the support from MEXT.

## 10. References

Adair, R.K. (1994). The Physics of Baseball, *Harper Perennial*, New York

Alaways, L.W., Mish, S.P. & Hubbard, M. (2001). Identification of release conditions and aerodynamic forces in pitched-baseball trajectories, *Journal of Applied Biomechanics*, Vol. 17, No.1, (2001), pp. 63-76

Alaways, L.W. & Hubbard, M. (2001). Experimental determination of baseball spin and lift, *Journal of Sports Sciences*, Vol. 19, No.5, (2001), pp. 349-358

ANSYS/LS-DYNA Theoretical Manual (2002), SAS IP Inc.

Chu, W.T., Wang, C.W. & Wu, J.L. (2006). Extraction of baseball trajectory and physics-based validation for single-view baseball video sequences, *IEEE International Conference on Multimedia and Expo*, ICME 2006, Art. No. 4036974, (2006), pp. 1813-1816

Frohlich, C. (1984). Aerodynamic drag crisis and its possible effect on the flight of baseballs, *American Journal of Physics*, Vol. 52, No.4, (1984), pp. 325-334

Hendee, S.P., Greenwald, R.M. & Crisco, J.J. (1998). Static and dynamic properties of various baseballs, *Journal of Applied Biomechanics*, Vol.14, No.4, (1998), pp. 390–400

Himeno, R., Sato, S. & Matsumoto, H. (1999). CFD study of the effect of seam on the flow around a baseball ball, *RIKEN Review, Focused on High Performance Computing in RIKEN*, No.25, (1999), pp. 124-127

Himeno, R. (2001). Computational Study of Influences of a Seam Line of a Ball for Baseball on Flows, *Journal of Visualization*, Vol. 4, No.2, (2001), pp. 197-207

* Corresponding Author

Jinji, T. & Sakurai, S. (2006). Direction of spin axis and spin rate of the pitched baseball, *Sports Biomechanics*, Vol. 5, No.2, (2006), pp. 197-214

Khuri, A.I. & Cornell, J.A. (1996). Response Surfaces; Design and Analysis, *Marcel Dekker*, New York, (1996)

Mehta, R. D. (1985). Aerodynamics of sports balls, *Annual Review of Fluid Mechanics*, Vol.17, (1985), pp. 151-189

Mish, S.P. & Hubbard, M. (2001). Design of a Full Degree-of-freedom Baseball Pitching Machine, *Journal of Sports Engineering*, Vol. 4, No.3, (2001), pp.123-133

Mizota, T., Kuba, H. & Okajima, A. (1995). Erratic Behavior of Knuckle Ball (1) Quasi-steady Flutter Analysis and Experiment, *Journal of Wind Engineering*, Vol. 62, No.62, (1995), pp. 3-13

Mizota, T., Kuba, H. & Okajima, A. (1995). Erratic Behavior of Knuckle Ball (2) Wake Field and Aerodynamic Forces, *Journal of Wind Engineering*, Vol. 62, No.62, (1995), pp. 15-22

Myers, R.H. & Montgomery, D.C. (1995). Response Surface Methodology: *Process and Product Optimization Using Designed Experiments*, John Wiley & Sons. Inc., (1995)

Nathan, A.M. (2008). The effect of spin on the flight of a baseball, *American Journal of Physics*, Vol. 76, No.2, (2008), pp. 119-124

Nicholls, R.L., Miller, K. & Elliott, B.C. (2003). Bat kinematics in baseball: implications for ball exit velocity and player safety, *Journal of Applied Biomechanics*, No.19, (2003), pp. 283-294

Nicholls, R.L., Miller, K. & Elliott, B.C. (2004). Modeling Deformation Behavior of the Baseball, *Journal of Applied Biomechanics*, Vol. 21, No.1, (2004), pp. 9-15

Nicholls, R.L., Miller, K. & Elliott, B.C. (2006). Numerical analysis of maximal bat performance in baseball, *Journal of Biomechanics*, Vol. 39, No. 6, (2006), pp. 1001-1009

Oda, J., Sakai, S., Yonemura, S., Kawata, K., Horikawa, S. & Yamamoto, H. (2003). Development research of intelligent pitching machine using neural network, *Transactions of the Japan Society of Mechanical Engineers*, Series C, Vol.69, No.678, (2003), pp.135-140, (in Japanese)

Sakai, S., Oda, J., Yonemura, S., Kawata, K., Horikawa, S. & Yamamoto, H. (2007). Research on the Development of Baseball Pitching Machine Controlling Pitch Type Ball Using Neural Network, *Journal of System Design and Dynamics*, Vol. 1, No.4, (2007), pp. 682-690

Sakai, S., Oda, J., Kawata, K. & Kitagawa, Y. (2007). Study on Throw Accuracy for Baseball Pitching Machine with Roller, *Transactions of the Japan Society of Mechanical Engineers*, Series C, Vol. 73, No.735, (2007), pp. 90-95, (in Japanese)

Sakai, S., Oda, J., Yonemura, S. & Sakamoto, J. (2008). Study on Impact Loading and Humerus Injury for Baseball, *Journal of Computational Science and Technology*, Vol. 2, No.4, (2008), pp. 609-619

Takahashi, M., Fujii, M. & Yagi, N. (2008). Automatic pitch type recognition from baseball broadcast videos, *10th IEEE International Symposium on Multimedia*, ISM 2008 , Art. No. 4741142, (2008), pp. 15-22

Todoroki, A., "RSMaker for Excel", 20. 05. 2010, Available from

http://todoroki.arrow.jp/ssoft/RSMkaisetsu.pdf

Watts, R.G. & Sawyer, E. (1975). Aerodynamics of Knuckleball, *American Journal of Physics*, Vol.43, No.11, (1975), pp. 961-963